RPE | Radiation Physics & Engineering
A Peer-Reviewed Journal
Published by K.N. Toosi University of Technology
http://rpe.kntu.ac.ir
Research Article

Radiation Physics and Engineering 2025; 6(4):55–64

Vacuum system design and pressure profile calculation for the accelerating tube of a tandem accelerator

Masoud Mohseni Kejani[a], Fereydoun Abbasi Davani[a], Farshad Ghasemi[b,*], Shahin Sanaye Hajari[b], Mohammad Lamehi Rachti[b]

[a] *Department of Radiation Application, Faculty of Nuclear Engineering, Shahid Beheshti University, P.O. Box 19839-69411, Tehran, Iran*
[b] *Physic and Accelerators Research School, Nuclear Science and Technology Research Institute, P.O. Box 14395-836, Tehran, Iran*

HIGHLIGHTS

- Poor vacuum conditions increase electron production, which lead to enhanced background radiation.
- Design of vacuum system for the gas-based charge exchange method in tandem accelerators.
- Determine optimal operating window for gas throughput and pumping speed in charge exchange region.
- Ensuring atomic gas density of 7.24×10^{16} cm^{-2} required for nearly 100% charge exchange efficiency.
- Effective range of pump speeds on charge exchange section and accelerating tubes was identified.

ABSTRACT

In tandem accelerators, charge exchange can be achieved using either foil-based or gas-based methods. This study presents the design of a vacuum system specifically for the gas-based charge exchange method in tandem accelerators, aiming to maintain optimal atomic gas density in the interaction region and minimize gas leakage toward the accelerating tubes. To achieve high charge exchange efficiency, precise design of the Beam Transfer Lines (BTL) is essential. In this study, the impact of length and diameter of the BTL on the pressure profile along the tube was investigated. A geometry was selected that concentrates gas in the interaction region while minimizing leakage into accelerating tubes. Subsequently, gas flow simulations were used to determine the optimal operating window for gas throughput and pumping speed in the charge exchange region, ensuring an atomic gas density of 7.24×10^{16} cm^{-2} required for nearly 100% charge exchange efficiency. Keeping the gas injection rate fixed, the effective range of pump speeds on charge exchange section and accelerating tubes was then identified to create a pressure ratio of about 10^{-3} mbar between the charge exchange section and accelerating tubes. Results showed that beyond a certain threshold, increasing pumping speed does not significantly reduce the pressure due to conductance limitations.

KEYWORDS

Tandem technique
Vacuum system
Pressure profile
Conductance
Optimal operating window

HISTORY

Received: 16 July 2025
Revised: 23 August 2025
Accepted: 17 September 2025
Published: Autumn 2025

1 Introduction

A proton beam has a wide range of applications in medical, industrial, and research fields. In medicine, it is used for ion therapy (Loap et al., 2024; Sterpin et al., 2024), radiopharmaceutical production (Boschi et al., 2017), and techniques such as boron neutron capture therapy (BNCT) (Dimov et al., 2003; Nakamura et al., 2022). In industry, the proton beam is employed in processes such as ion implantation (Upadhyay et al., 2016) and neutron production (Zmeškal et al., 2023). In scientific research, it is utilized to improve material properties (Zhou et al., 2004) and conduct material analysis (Hietel et al., 1996; Mouchard et al., 2024).

Among various types of accelerators, the electrostatic tandem accelerator (Van de Graaff, 1960) is considered a suitable option for generating high-energy proton beams for material analysis applications due to its unique features, such as high beam energy resolution (in the 10^{-4} beam energy range (Uchiyama et al., 1991)). In this type of accelerator, a negative ion is first generated in the ion source. After acceleration through the low-energy section of the accelerating tube, the beam enters the charge exchange section via Negative Beam Transfer Line (NBTL),

*Corresponding author: fsghasemi@aeoi.org.ir

https://doi.org/10.22034/rpe.2025.534992.1284

where it undergoes charge transformation from negative to positive (Hotchkis et al., 2013). The beam then enters the high-energy section of the accelerating tube via Positive Beam Transfer Line (PBTL) and it will accelerate again. As a result, for hydrogen ion beams, this technique enables achieving twice the energy relative to the terminal voltage (Van de Graaff, 1960).

One of the main differences between this type of accelerator and single-stage electrostatic accelerators is the charge exchange section. In this section, negative ions are converted into positive ions using either a carbon foil (Shima et al., 2001; von Reden et al., 2007; Gulley et al., 1996) or a gas (Makarov et al., 2015; Kolesnikov et al., 2020; Saitoh et al., 2009). Due to its better stability at high currents, the gas-based charge exchange is more commonly used in applications such as beam analysis (Burducea et al., 2017; Maruta et al., 2024) or ion implantation (Burducea et al., 2017; O'Connor and Tokoro, 1993; Mas-Ruiz et al., 2023). In the gas-based method, the absence of a separating window allows the gas to be injected directly into the beamline to provide a suitable atomic density for charge exchange. Improper vacuum system design in the charge exchange section and accelerating tubes fails to establish the required atomic gas density along the beam path, causing gas leakage into both the high-energy and low-energy sections. This leakage compromises the necessary vacuum level (around 10^{-6} mbar (Hellborg, 2005)) in these areas and disrupts optimal system performance. Therefore, the vacuum system is a key factor in the performance and stability of tandem accelerators. Achieving a proper vacuum level is essential to reduce beam scattering and prevent energy loss due to interactions between ions and residual gas molecules. Such interactions can reduce beam resolution, lower beam transmission efficiency, and decrease beam current. Additionally, poor vacuum conditions increase the probability of secondary electron production, which can lead to enhanced background radiation.

The Physics and Accelerators Research School (PARS) at the Nuclear Science and Technology Research Institute (NSTRI) is active in the development of both radiofrequency (Aghayan et al., 2021; Zarei et al., 2017, 2023; Kejani et al., 2019) and electrostatic accelerators (Nazari et al., 2020; Mirzaei et al., 2025; Shirshekan et al., 2024; Hasanpour et al., 2022). At NSTRI, a high-voltage power supply based on parallel-fed CockcroftWalton structure has been designed and constructed. This system comprises 34 cascade stages housed in an insulating gas-filled chamber and is capable of producing 1.7 MV maximum. Currently, the design of a tandem accelerator for beam analysis and ion implantation applications is in progress, using this high-voltage power supply. In this system, nitrogen gas is selected for charge exchange due to its high charge exchange cross-section at the desired proton beam energy (Heinemeier et al., 1976).

This paper focuses on the vacuum system design for the accelerating tube of this tandem accelerator and presents the pressure profile calculation along the beam path. Initially, the gas transport behavior within the charge exchange cell is discussed, and the designed geometry for the charge exchange section is introduced. This is followed by a review of the relevant charge exchange interaction equations and cross-section data, along with a description of the problem-solving approach and solution methodology. Finally, based on the simulation results, an optimized vacuum system is proposed to fulfill the operational requirements of the tandem accelerator.

2 Gas transport behavior in the charge exchange cell and geometric design

The charge exchange section in a tandem accelerator is situated between the low-energy and high-energy sections of the accelerating tube and is primarily responsible for converting negative ions into positive ones. In a gas-based charge exchange system, an appropriate gas is injected to achieve the required atomic gas density for efficient charge exchange processes. As the atomic gas density increases, the interactions between negative ions and gas molecules rises, leading to a higher conversion rate of negative ions to positive ones. However, since the ion acceleration process within the accelerating tube demands a high vacuum level (in order of 10^{-6} mbar (Heinemeier et al., 1976)) controlling gas leakage from the charge exchange section into the accelerating tube becomes a major challenge. One possible solution to prevent gas leakage is to use a physical window to isolate the charge exchange region from the accelerating tube. However, this method presents significant disadvantages, as placing a window in the beam path can severely attenuate the ion beam intensity, thereby reducing the overall system efficiency. Therefore, the charge exchange section should be designed to maximize the gas number density along the beam path using the lowest possible gas injection rate, while also ensuring minimal gas leakage into the accelerating tube. Accordingly, the proper geometric design of various components, along with the selection of an appropriate vacuum pump speed, is essential for achieving the desired vacuum conditions in the accelerating tube. A schematic of the tandem accelerator is presented in Fig. 1.

Depending on the pressure conditions, the gas transport behavior can be described by three regimes, which are characterized by the Knudsen number (Kn). The Knudsen number is defined as $Kn = \lambda/d$, where d is the characteristic dimension (e.g., tube diameter) and λ is the mean free path of gas molecules (Hellborg et al., 2005). Based on the Kn value, the flow is categorized into molecular flow ($Kn > 1$), transitional flow ($0.01 < Kn < 1$), and viscous flow ($Kn < 0.01$) (O'Hanlon, 2003). In the present study, the operating pressure inside the accelerating tube corresponds mainly to the molecular flow regime, which is the relevant regime for the vacuum system design considered here.

The geometry of the charge exchange section and the pressure gradient along the beam path determine the extent of gas leakage into the accelerating tube. This effect is quantified by the conductance (C), which represents the capacity of a given geometry to allow gas flow under a pressure difference. Conductance is defined as $C = Q/(P_2 - P_1)$, where Q is the gas throughput

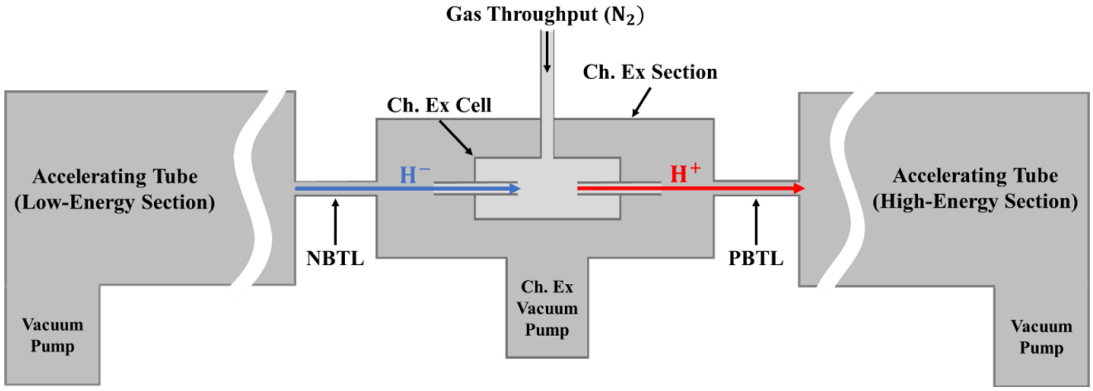

Figure 1: Schematic of the tandem accelerator.

($Pa.m^3.s^{-1}$), and P_1 and P_2 are the pressures at two points (Pa) (O'Hanlon, 2003). The Knudsen number therefore provides the criterion for selecting the appropriate conductance formulation, as the dependence of conductance on geometry differs between molecular, transitional, and viscous regimes. For molecular flow in a long cylindrical tube, C is proportional to d^3/L, where d is the tube diameter and L is its length (Hellborg et al., 2005). Therefore, to suppress gas leakage and achieve the required vacuum level, the charge exchange section must be designed with an optimized geometry that minimizes conductance between the charge exchange region and the accelerating tube.

Gas molecules collide with the walls more often than with one another in the free molecular flow regime. This kind of flow can be simulated in two main ways. The first is the Direct Simulation Monte Carlo (DSMC) method (Prasanth and Kakkassery, 2008), which follows the paths of numerous particles that are dispersed at random throughout the system. The second is the Angular Coefficient method, which integrates the flux received on a surface from every other surface in its line of sight to determine the gas flow (Ossipov, 1997). The Angular Coefficient method's primary advantages over DSMC are its faster computation and the removal of statistical scatter from the results. The Angular Coefficient method is used in the Free Molecular Flow interface of COMSOL Multiphysics software (https://www.comsol.com/) to solve gas flow problems. This interface is capable of calculating flux, pressure, and molecular number density at specified points, along defined paths, and within various regions inside boundary surfaces.

The geometry of the charge exchange system was optimized in a separate study by the authors of this paper, as reported in reference (Kejani et al., 2025). Free Molecular Flow interface of COMSOL Multiphysics software was used to perform accurate calculations for this optimization. The charge exchange section has its own vacuum pump, as illustrated in Fig. 1, and each of the low-energy and high-energy sections of the accelerating tube have their own vacuum pump. In this optimization the vacuum pump speed for all three sections was set at 300 $L.s^{-1}$, and a nitrogen gas throughput of 10 standard cubic centimeters per minute (SCCM) was taken into account. The gas temperature was assumed to be constant at 20 °C under steady-state conditions. Finally, the optimized dimensions of the charge exchange section, reflecting the results of this optimization, are presented in reference (Kejani et al., 2025).

In the charge exchange cell designed for converting an H^- beam to H^+ at an energy of 1.7 MeV, it is essential to consider all interactions that result in proton production following the collision of H^- ions with nitrogen gas molecules. To achieve this, two primary approaches for converting H^- to H^+ are considered: 1) Direct Conversion: H ions directly lose two electrons in a single collision, resulting in the formation of H^+ ions; 2) Indirect Conversion: H ions first undergo a single-electron detachment to become neutral hydrogen atoms (H^0), which subsequently lose another electron in a following collision to form H^+ ions. To calculate the number of each interaction ($N_{qq'}$), the Eq. (1) is used:

$$N_{qq'} = N_q.\sigma_{qq'}.n_{gas}.x \tag{1}$$

where N_q is the number of incident particles, $\sigma_{qq'}$ is the interaction cross-section (in cm^2), q and q' are the initial and final charge state of particles, n_{gas} is the atomic density of gas molecules (in cm^{-3}) and x is the interaction length (in cm). Accordingly, the interaction rates for each of two approaches (direct and indirect) are determined by Eqs. (2) and (3):

$$\text{Direct conversion: } N_{-11} = N_{-1}.\sigma_{-11}.n_{gas}.x \tag{2}$$

$$\text{Indirect conversion: } N_{-11} = N_{-1}.(\sigma_{-10}.\sigma_{01}).(n_{gas}.x)^2 \tag{3}$$

Therefore, the interaction rate within the charge exchange cell for a given gas and energy of ions is influenced by the cell's geometry (which affects the interaction length), the gas number density and the interaction cross section.

In calculating the atomic number density of the gas required in the charge exchange cell, it is important to use accurate values for the interaction cross sections. Considering the maximum voltage that can be supplied by the designed power supply, the energy of the H^- beam upon entering the charge exchange section will be 1.7 MeV. Due to the high energy resolution of electrostatic accelerators (10^{-4} of the beam energy (Uchiyama et al., 1991)), the energy spread resulting from the high-voltage power supply can be considered negligible.

Table 1: Energy ranges (in keV) for interaction cross-sections reported in various references.

	σ_{-11}	σ_{-10}	σ_{01}
(Heinemeier et al., 1976)	100 - 500	100 - 500	-
(Allison, 1958)	5 - 40	4 - 30	4 - 10^3
(Schryber, 1967)	-	-	1040 - 4180
(Barnett and Reynolds, 1958)	-	-	10 - 10^3
(Barnett et al., 1977)	5 - 104	0.2 - 1.5 × 10^4	4 - 10^4
(Toburen et al., 1968)	-	-	100 2.5 × 10^3
(Lichtenberg et al., 1980)	44 - 227	50 - 227	-
(Dmitriev et al., 2010, 1995)	-	300	300, 700
(Stier and Barnett, 1956)	-	4 - 30	-
(Welsh et al., 1967)	-	-	1027, 2440
(Ormrod and Michel, 1971)	-	-	5 - 80
(Kovacs, 1967)	200 - 500	200 - 500	-
(Pilipenko and Fogel, 1962)	-	-	5 - 40
(Tawara et al., 1990)	-	10 - 1 × 10^4	-
(Puckett et al., 1969)	-	-	150 - 400
(Noda, 1976)	-	-	0.3 - 5
(Miethe et al., 1982)	-	-	0.14 - 5
(Fogel et al., 1957)	5 - 40	-	5 - 40

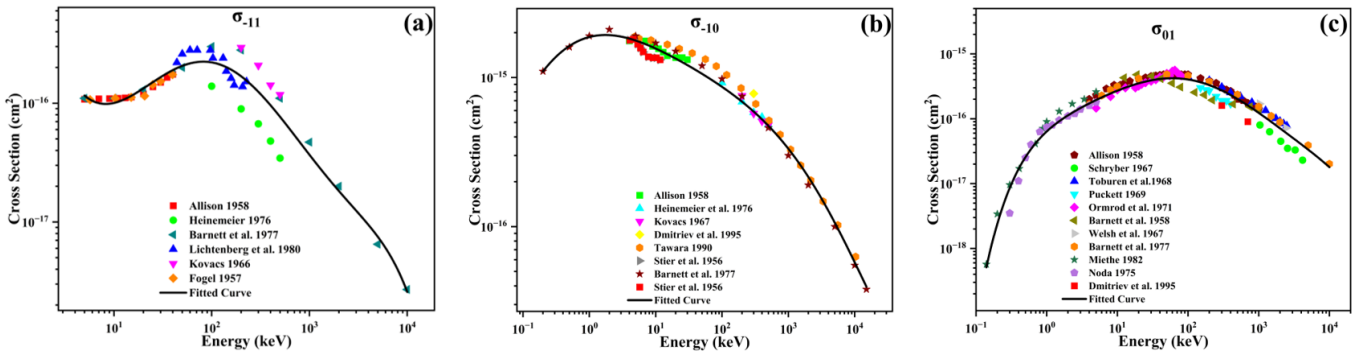

Figure 2: Cross section of charge exchange interactions a) σ_{-11}, b) σ_{-10}, c) σ_{01}.

In this study, the cross-section values for charge exchange processes were obtained using fitted functions provided in reference (Kejani et al., 2025). These functions were derived by applying polynomial fitting to experimental data published in various references, enabling the extrapolation of cross-section values at the energy of 1.7 MeV. Details of the fitting procedure and its statistical accuracy are available in the reference (Kejani et al., 2025). Table 1 presents the cross sections used for both direct and indirect charge exchange interactions, and Fig. 2 illustrates the agreement between the fitted curves and the published experimental data for the specified energy.

The efficiency (η) of the charge exchange cell, defined as the ratio of the number of H^+ ions to the number of H^- ions. Therefore, the efficiency equations for both direct and indirect conversion methods of H^- to H^+ are calculated using Eqs. (4) and (5), respectively:

$$\text{Direct conversion: } \eta_1 = \sigma_{-11}.n_{gas}.x \quad (4)$$

$$\text{Indirect conversion: } \eta_2 = (\sigma_{-10}.\sigma_{01}).(n_{gas}.x)^2 \quad (5)$$

Considering the cross-section values for each of the direct and indirect conversion interactions, the conversion efficiency of H^- ions to H^+ can be analytically calculated for the two primary pathways. In these calculations, due to the high energy resolution of the selected accelerator, the energy spread is neglected. Therefore, the beam energy is assumed to be constant at 1.7 MeV, and the efficiency equations are derived accordingly.

By solving the corresponding equations for an ideal efficiency of 100%, the required gas thickness (ngas.x) for complete conversion of H^- ions to H^+ was determined. For the direct pathway (simultaneous removal of two electrons from H^-), the required gas thickness was calculated to be 7.24×10^{16} cm^{-2}, while for the indirect pathway (sequential removal of two electrons from H^- and then H^0), it was found to be 7.17×10^{15} cm^{-2}.

Although the indirect pathway requires a smaller gas thickness for H^- to H^+ conversion, in practice, secondary interactions within the gas environment of the charge exchange cell may lead to the loss of H^+ or H^0 particles. These include processes such as electron attachment to H^+ (converting it back to H^0), or even reverse conversion to H^-. While the cross-sections of these secondary interactions are smaller than those of the primary processes (Barnett et al., 1977; Toburen et al., 1968; Welsh et al., 1967), they can slightly reduce the overall efficiency under

real operating conditions.

Therefore, to ensure effective and complete conversion of the H^- beam to H^+, the higher gas thickness corresponding to the direct pathway is adopted as the design basis. This conservative approach ensures that even in the presence of unfavorable interactions, sufficient gas density is maintained to achieve high efficiency.

Accordingly, in the design of the charge exchange cell, this value is considered the required gas thickness to achieve approximately 100% efficiency, and all other geometric and operational parameters are determined based on this value.

3 Simulation Methodology and Problem-Solving Approach

In the design of the vacuum system for the accelerating tube of a tandem accelerator, the primary objective is to achieve the highest possible atomic gas density in the beam interaction region with the minimum gas injection rate. This ensures maximum charge exchange efficiency while preventing gas leakage into the low- and high-energy sections of the accelerating tube and maintaining the required vacuum conditions throughout the system. To accomplish this goal, an optimized geometric design and the careful selection of operational parameters -such as gas injection rate and pumping speed- are essential.

Although various combinations of operational parameters can provide the required gas density, the optimal design focuses on achieving the desired performance conditions with the lowest possible gas throughput and minimal pumping speed. This approach reduces gas consumption, extends the service life of vacuum components, enhances beam transmission efficiency, reduces background radiations, and improves the overall stability of system operation.

One of the critical factors affecting the pressure profile inside the accelerating tube is the geometry of the Beam Transfer Lines (BTL) between the charge exchange section and the accelerating tubes. Therefore, prior to performing calculations dependent on gas throughput and pumping speed, this section was analyzed as a key structural element. Specifically, the BTL must be designed to minimize gas leakage from the charge exchange section into the accelerating tubes.

In this analysis, the length and diameter of the BTL (see Fig. 1) were varied under fixed gas throughput and pumping speed conditions, and their impact on the pressure profile along the tube was evaluated. The results enabled the selection of optimal dimensions for the BTL to ensure both minimal gas leakage into the accelerating tubes and consequently effective ion beam transmission. Since the charge exchange cross-sections for H^- are much larger than those for H^+, the vacuum quality in the low-energy section connected to the NBTL is more critical. Nevertheless, to adopt a conservative design strategy, the PBTL was treated under the same vacuum requirements as the NBTL, ensuring that suitable vacuum conditions are achieved throughout the entire accelerating tube.

An appropriate design of the charge exchange cell is achieved when the gas throughput and pumping are configured such that gas delivery to the interaction region is effective yet limited. The system's overall performance is greatly influenced by these parameters since they have a direct impact on the pressure profile along the beamline and the distribution of atomic gas density.

Based on the theoretical relationships between pressure, gas throughput, pumping speed, and conductance of the vacuum path, the pressure can be expressed as a function of the gas injection rate and the effective pumping speed. The pressure (P) is related to the effective pumping speed (S_{eff}) and the gas throughput (Q) based on Eq. (6). And on the other hand, the relationship between effective pumping speed (S_{eff}), pump speed (S), and conductance (C) is given by Eq. (7):

$$P = \frac{Q}{S_{eff}} \tag{6}$$

$$\frac{1}{S_{eff}} = \frac{1}{S} + \frac{1}{C} \tag{7}$$

Under ideal conditions, increasing the pump speed leads to a reduction in pressure. However, in reality, the limited conductance (C) of the vacuum path imposes a constraint such that, in the molecular flow regime (at low pressures), the system's performance becomes predominantly conductance-limited. When $C \ll S$, further increasing the pumping speed has little impact on pressure reduction, and the system behavior is governed primarily by the conductance.

Accordingly, the optimal design strategy is to select the gas throughput at an appropriate value that achieves the desired atomic gas density without requiring the use of excessively high-capacity pumps. To this end, a range of gas flow rates (Q) and pumping speeds (S) was analyzed through parametric simulations to identify the "Optimal Operating Window" for the vacuum system. This window includes the set of parameter combinations that ensure high charge exchange efficiency while maintaining suitable pressure levels in three critical regions: the charge exchange section, the low-energy section, and the high-energy section of the accelerating tube. To ensure the atomic gas density required for nearly 100% charge exchange efficiency (corresponding to 7.24×10^{16} cm^{-2}), the gas throughput was first determined based on this target density. Once the optimal gas throughput was established, it was held constant while the pumping speeds at two key locations in the system (the charge exchange section and the accelerating tube) were varied.

The resulting pressure profile along the accelerating tube was calculated for each case. A pressure differential on the order of 10 mbar (Wiebert et al., 1995; Persson et al., 2003; Hellborg et al., 2002; Kiisk et al., 2004) between the charge exchange section and at the entrance of the low-energy section of the accelerating tube was defined as the final design goal. This pressure drop was achieved by tuning the pumping speeds on both sides while maintaining the gas throughput constant. Based on these simulations, the optimal operating window for both gas

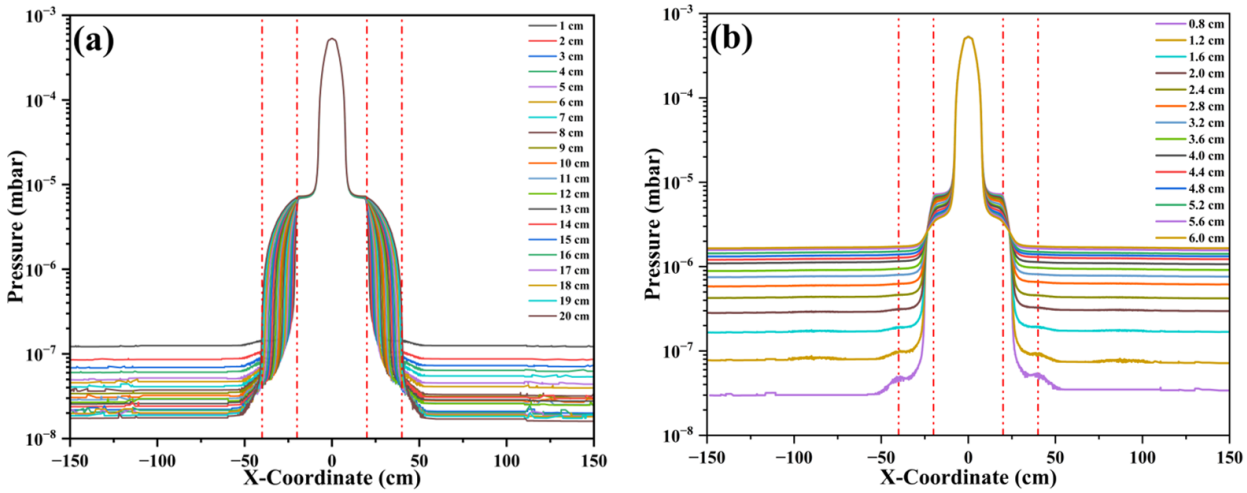

Figure 3: Pressure profile along the beam path, a) BTL length, b) BTL diameter.

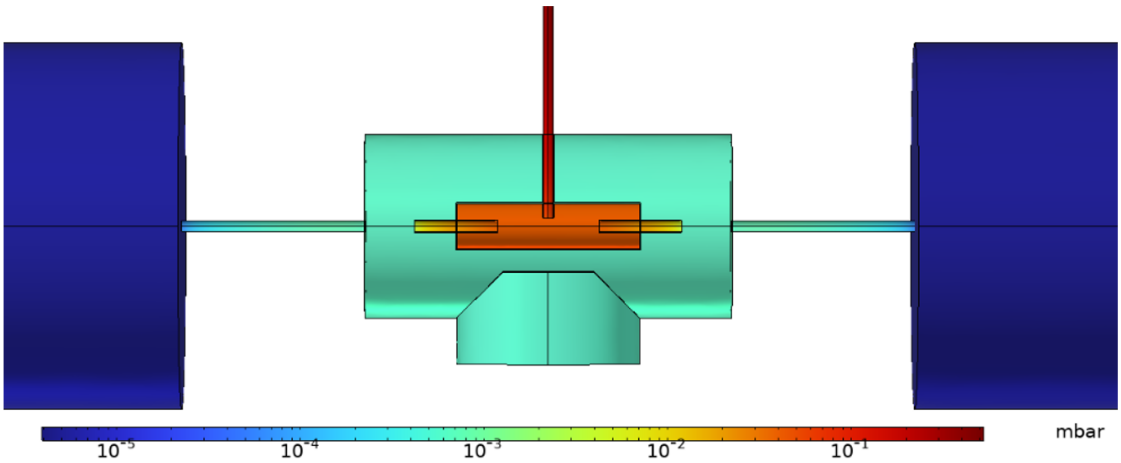

Figure 4: Pressure distribution for the final geometry.

throughput and the pumping speeds in each region was identified, ensuring that the system maintains sufficient gas density for efficient charge exchange while minimizing gas leakage and the need for high-capacity or high-cost pumps.

In total, 200 simulation cases were conducted: 100 cases for determining the optimal gas injection rate required to achieve the desired atomic gas density, and another 100 cases for identifying the optimal operational window for the vacuum pump speeds. These computations were performed using the High-Performance Computing (HPC) system at the Nuclear Science and Technology Research Institute (NSTRI). The entire process required approximately 120 hours of computational time, utilizing 52 CPU cores and about 100 GB of RAM. The geometry was fully meshed with approximately 950 k elements.

4 Results

To produce an appropriate pressure profile along the accelerating tube and to ensure the required atomic gas density in the charge exchange section, the design of the BTL is important. To evaluate the effect of this section, the impact of the length and diameter of the BTL on the pressure profile was investigated. The simulation results are presented in Fig. 3, demonstrating that these two parameters significantly influence the pressure profile in the beam path. Based on this analysis, the optimal values of the length and diameter of the BTL were determined to be 20 cm and 1.2 cm, respectively. In this design, the transverse beam size was assumed to be approximately 1 cm. Figure 4 illustrates the pressure distribution for the optimized geometry.

With the optimized geometry established, various combinations of gas throughput and pumping speeds in the charge exchange section were analyzed to determine the conditions required to achieve the gas thickness for efficient charge exchange. Gas throughputs ranging from 10 to 100 SCCM and pumping speeds between 10 and 100 L.s^{-1} (in steps of 10 for both) were considered. For each case, the resulting gas thickness within the charge exchange section was calculated and compared with the desired values. The outcomes are presented in Figure 5, where the optimal operating window (defined as an atomic gas density between 6×10^{16} and 8×10^{16} cm^{-2}) is highlighted.

Although the optimal density for achieving nearly 100% charge exchange efficiency was calculated to be 7.24×10^{16} cm^{-2}, a broader range was adopted in the simulations to reflect potential real-world deviations. This includes uncertainties such as pressure instabilities, temperature fluctuations, and atomic interactions that were not considered in the calculations (such as proton loss due to neutralization via electron capture or the conversion of neutral atoms into negative ions). By defining an optimal operating window rather than a single target value, the design ensures improved stability of the vacuum system under practical operating conditions. The values of gas thickness corresponding to different combinations of gas throughputs and the charge exchange (Ch. Ex) pump speed are presented in Fig. 5.

Based on Fig. 5, it can be observed that the gas thickness initially decreases with an increase in pumping speed; however, after a certain point, the gas thickness stabilizes. Therefore, in this scenario, the required gas thickness becomes proportional to the gas throughput. According to Fig. 5, the optimal gas throughput for the charge exchange section was chosen to be 25 SCCM.

In the next step, with the gas throughput set to 25 SCCM, variations in the pumping speeds of the accelerating tube and the charge exchange section were made, and the pressure profile along the accelerator tube was analyzed. Pumping speeds ranged from 10 to 100 L.s^{-1} in increments of 10 units, and the pressure ratio between the charge exchange section and the low-energy section of the accelerator tube was calculated. Since the pressure ratio between these two points should be around 10^{-3} (Wiebert et al., 1995; Persson et al., 2003; Hellborg et al., 2002; Kiisk et al., 2004) to ensure the necessary vacuum for ion accelerating and prevent operational issues, the pressure ratio was calculated and analyzed for all different cases. The results are presented in Fig. 6. The pressure ratio range between 9.0×10^{-4} and 1.0×10^{-3} is defined as the optimal operating window for the system.

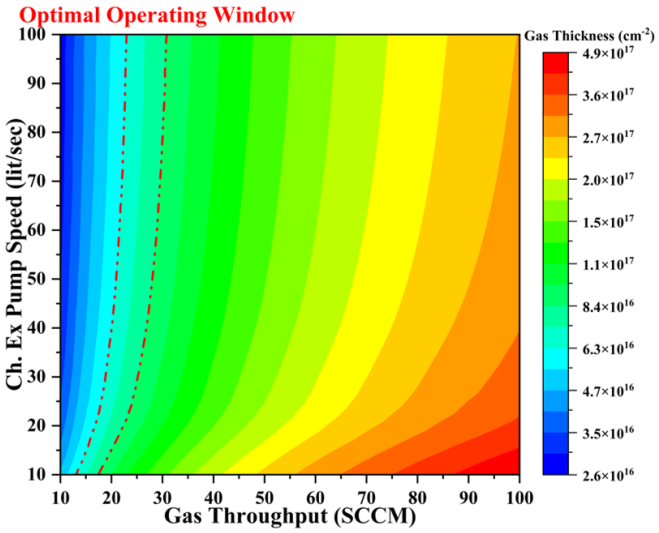

Figure 5: The values of gas thickness corresponding to different combinations of gas throughputs and the Ch. Ex pump speed.

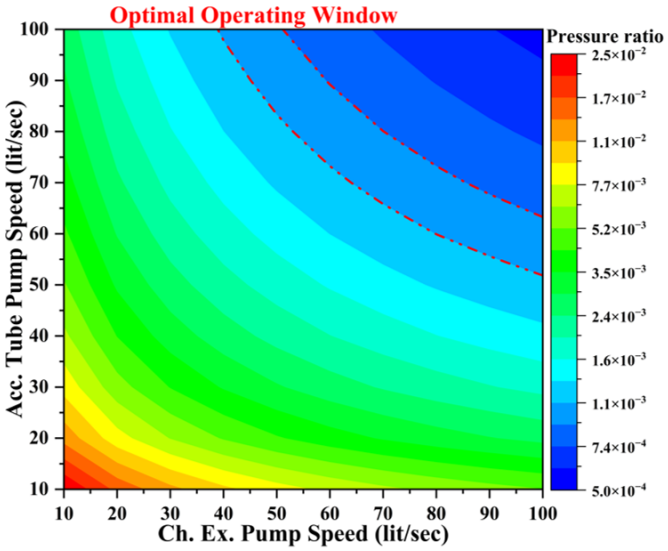

Figure 6: The pressure ratio of Ch. Ex. section and L.E section of accelerating tube for different pump speed variations.

Figure 7 presents the diagram of the vacuum system designed for the tandem accelerator. At the beginning of the beamline, the ion source is placed and equipped with a dedicated vacuum pump to ensure optimal conditions for H^- beam production and extraction. The beam then enters the low-energy section of the accelerating tube, where a turbomolecular pump maintains the required vacuum, and a pressure gauge with a display unit allows real-time monitoring. After passing through the NBTL, the beam enters the charge exchange section. In the charge exchange section, nitrogen gas is injected into the charge exchange cell using a variable leak valve. The internal pressure of the chamber is continuously monitored by a vacuum gauge connected to a display unit. In charge exchange section, a turbomolecular pump with magnetic coupling is used to avoid any physical or electrical connection between the high-voltage components and the pump's motor. This eliminates the risk of stray currents potentially introduced via power cables, shafts, or bearings, which could be hazardous in such environments. Following the conversion of H^- to H^+, the beam continues through the PBTL into the high-energy section of the accelerating tube, which also includes a vacuum gauge for monitoring and a turbomolecular pump at the tubes exit to maintain proper vacuum conditions. Finally, the beam reaches a vacuum chamber dedicated to experimental measurements. It has to be noted that, all turbomolecular pumps in the system are backed by rotary pumps to handle initial pumping and ensure proper operation.

5 Conclusions

In this study, the effect of the length and diameter of the BTL on the pressure profile within the tandem tube was investigated. By analyzing the influence of these two parameters, a configuration was selected that concentrates gas in the interaction region while preventing its leakage into the low- and high-energy sections of the accelerating

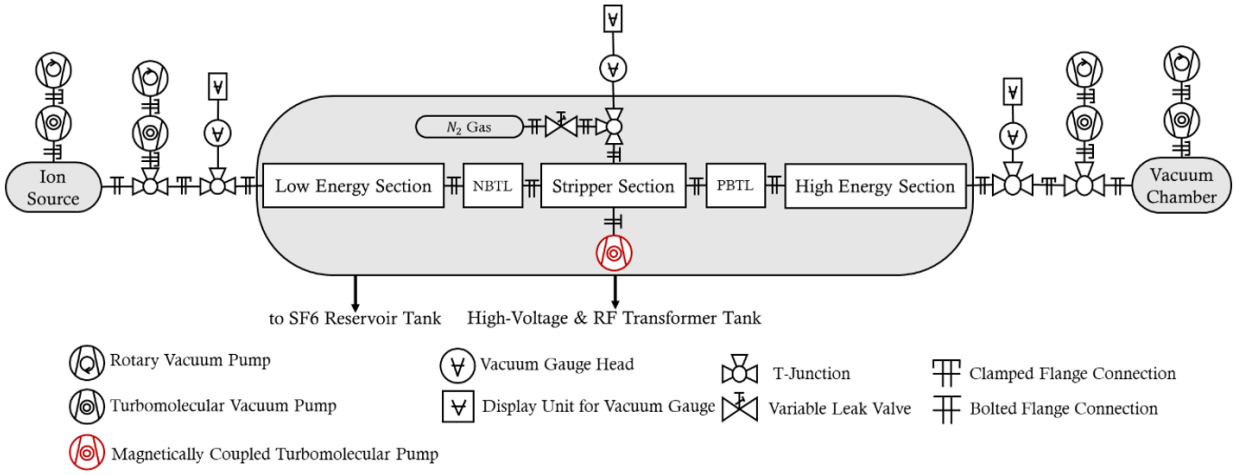

Figure 7: Diagram of the vacuum system for the accelerating tube.

tubes.

Subsequently, the optimal operating window for gas throughput and pumping speed in the charge exchange section was determined to achieve a sufficient atomic gas density (equal to 7.24×10^{16} cm^{-2}). Then, with the gas throughput fixed at its optimal value of 25 SCCM, the vacuum pump speeds on charge exchange section and accelerating tubes were varied to achieve the design target (a pressure ratio of approximately 10 mbar). Based on the results, the optimal operating window for the pumping speeds in each section was identified, allowing efficient system performance without relying on excessively large or costly pumps.

The results also indicated that increasing the pumping speeds improves the pressure conditions only up to a certain point. Beyond this limit, no significant change in pressure is observed, which is attributed to the limited conductance of the vacuum paths. Therefore, optimal vacuum system design requires simultaneous consideration of both pumping capacity and conductance.

Overall, the findings of this work demonstrate that with proper geometric design, targeted gas injection control, and optimized pump selection, it is possible to establish a stable, efficient, and cost-effective vacuum environment for tandem accelerator systems.

Conflict of Interest

The authors declare no potential conflict of interest regarding the publication of this work.

Funding

The authors declare that no funds, grants, or other financial support were received during the preparation of this manuscript.

References

Aghayan, M., Masoudi, S. F., Ghasemi, F., et al. (2021). Development of a novel approach for construction of high gradient braze-free S-band cavities. *Scientific Reports*, 11(1):18840.

Allison, S. K. (1958). Experimental results on charge-changing collisions of hydrogen and helium atoms and ions at kinetic energies above 0.2 kev. *Reviews of Modern Physics*, 30(4):1137.

Barnett, C., Ray, J., Ricci, E., et al. (1977). Atomic data for controlled fusion research. Technical report, Oak Ridge National Lab.(ORNL), Oak Ridge, TN (United States).

Barnett, C. and Reynolds, H. (1958). Charge exchange cross sections of hydrogen particles in gases at high energies. *Physical Review*, 109(2):355.

Boschi, A., Martini, P., Pasquali, M., et al. (2017). Recent achievements in Tc-99m radiopharmaceutical direct production by medical cyclotrons. *Drug Development and Industrial Pharmacy*, 43(9):1402–1412.

Burducea, I., Ghiţă, D., Sava, T., et al. (2017). Tandem accelerators in Romania: Multi-tools for science, education and technology. In *AIP Conference Proceedings*, volume 1852, page 060001. AIP Publishing LLC.

Dimov, G., Bel'chenko, Y. I., Krainov, G., et al. (2003). Tandem accelerator with vacuum insulation for boron-neutron-capture therapy and detection of explosives by resonance absorption of γ-rays. *Atomic Energy*, 94(2):116–119.

Dmitriev, I., Teplova, Y. A., Belkova, Y. A., et al. (2010). Experimental electron loss and capture cross sections in ion–atom collisions. *Atomic Data and Nuclear Data Tables*, 96(1):85–121.

Dmitriev, I., Teplova, Y. A., and Fainberg, Y. A. (1995). An experimental study of single electron loss cross sections for hydrogen atoms and negative hydrogen ions in various media. *Zh. Eksp. Teor. Fiz*, 107:55–61.

Fogel, I. M., Ankudinov, V., and Slabospitskii, R. (1957). Loss of 2 electrons in single collisions between negative hydrogen IONS and molecules of gases. *SOVIET PHYSICS JETP-USSR*, 5(3):382–390.

Gulley, M., Keating, P., Bryant, H., et al. (1996). Measurement of H-, H 0, and H+ yields produced by foil stripping of 800-MeV H- ions. *Physical Review A*, 53(5):3201.

Hasanpour, O., Abbasi Davani, F., Ghasemi, F., et al. (2022). Replacement of SF with N/CO in design of a parallel-fed voltage multiplier for electrostatic accelerator. *Radiation Physics and Engineering*, 3(2):17–25.

Heinemeier, J., Hvelplund, P., and Simpson, F. (1976). Collisional detachment cross sections for H-and He-at high energies. *Journal of Physics B: Atomic and Molecular Physics*, 9(15):2669.

Hellborg, R. (2005). *Electrostatic accelerators*. Springer.

Hellborg, R., Hākansson, K., Faarinen, M., et al. (2002). Mechanical design of the recirculating, terminal pumping in the lund pelletron, and experimental experience. *Pramana*, 59(5):725–737.

Hellborg, R., Kiisk, M., Persson, P., et al. (2005). Vacuum in an accelerator systemcalculations and measurements. *Vacuum*, 78(2-4):427–434.

Hietel, B., Menzel, N., and Wittmaack, K. (1996). Rbs control of the proton fluence in external PIXE analysis using a he atmosphere. *Nuclear Instruments and Methods in Physics Research Section B: Beam Interactions with Materials and Atoms*, 109:139–143.

Hotchkis, M., Child, D., Fink, D., et al. (2013). Sulphur hexafluoride as a stripper gas for tandem accelerators. *Nuclear Instruments and Methods in Physics Research Section B: Beam Interactions with Materials and Atoms*, 302:14–18.

Kejani, M. M., Ghasemi, F., Davani, F. A., et al. (2019). Multiphysics analysis of side-coupled RF cavity. *Journal of Instrumentation*, 14(07):P07001.

Kejani, M. M., Ghasemi, F., Davani, F. A., et al. (2025). Design and optimization of charge exchange cell for high energy H- to H+ conversion. *International Journal of Hydrogen Energy*, 102:1367–1376.

Kiisk, M., Hellborg, R., Persson, P., et al. (2004). The charge state distribution of Be, C, Cl and Al ions at the Lund Pelletron accelerator with the recently modified terminal pumping in use. *Nuclear Instruments and Methods in Physics Research Section A: Accelerators, Spectrometers, Detectors and Associated Equipment*, 521(2-3):299–305.

Kolesnikov, Y. A., Koshkarev, A., Taskaev, S. Y., et al. (2020). Diagnostics of the Efficiency of a Gas Stripping Target of a Tandem Accelerator with Vacuum Insulation. *Instruments and Experimental Techniques*, 63(3):310–314.

Kovacs, I. (1967). One and two electron loss cross sections of H- ions in CO2 or N2 gas. *Nuclear Instruments and Methods*, 51(2):224–228.

Lichtenberg, W., Bethge, K., and Schmidt-Bocking, H. (1980). Electron-loss cross sections for negative ions at high energies. *Journal of Physics B: Atomic and Molecular Physics*, 13(2):343.

Loap, P., De Marzi, L., Decroocq, J., et al. (2024). Proton therapy reduces the effective dose to immune cells in mediastinal hodgkin lymphoma patients. *International Journal of Particle Therapy*, 13:100110.

Makarov, A., Ostreinov, Y., Taskaev, S., et al. (2015). Modification of the argon stripping target of the tandem accelerator. *Applied Radiation and Isotopes*, 106:53–56.

Maruta, K., Toyama, S., Miwa, M., et al. (2024). Development of a multimodal ion-beam-analysis system for the 1-MV tandem Pelletron accelerator installed at Tohoku University. *Nuclear Instruments and Methods in Physics Research, Section B: Beam Interactions with Materials and Atoms*, 554:165414.

Mas-Ruiz, J., Marín-Lámbarri, D., Sandoval-Hipólito, S., et al. (2023). Monoisotopic targets production from atomic and molecular positive ion implantation in a tandem accelerator at low energies. In *Journal of Physics: Conference Series*, volume 2619, page 012010. IOP Publishing.

Miethe, K., Dreiseidler, T., and Salzborn, E. (1982). Charge transfer of hydrogen atoms in N2 and in caesium vapour. *Journal of Physics B: Atomic and Molecular Physics*, 15(17):3069.

Mirzaei, H., Sanaye, S., Yadollahzadeh, B., et al. (2025). Development and performance analysis of the 200 keV Cockcroft-Walton ion accelerator. *Results in Physics*, 68:108089.

Mouchard, Q., Hazim, M., Koumeir, C., et al. (2024). New experimental measurements of X-ray emissions induced by protons of several tens of MeV on elements with Z= 22 to Z= 79: Toward quantitative high-energy PIXE. *Radiation Physics and Chemistry*, 221:111777.

Nakamura, R., Hino, M., Tanaka, H., et al. (2022). Conceptual design of a target station using a 30-MeV cyclotron accelerator for the basic study of boron neutron capture therapy at KURNS. *Nuclear Instruments and Methods in Physics Research Section A: Accelerators, Spectrometers, Detectors and Associated Equipment*, 1042:167425.

Nazari, M., Ghasemi, F., Abbasi, F., et al. (2020). Design and simulation of a 1 MeV, 100 mA parallel-fed capacitive coupled cascade industrial accelerator. *Journal of Instrumentation*, 15(01):T01001.

Noda, N. (1976). Electron stripping of he and h in helium, hydrogen and nitrogen gases from 0.2 keV to 5.0 keV. *Journal of the Physical Society of Japan*, 41(2):625–632.

O'Connor, J. P. and Tokoro, N. (1993). The Use of Negative Ions in Ion Implantation with Tandem High Energy Accelerators. *MRS Online Proceedings Library (OPL)*, 316:649.

O'Hanlon, J. F. (2003). *A user's guide to vacuum technology*. John Wiley & Sons.

Ormrod, J. and Michel, W. (1971). Charge equilibrium fractions and charge-exchange cross sections for fast ions in nitrogen and argon. *Canadian Journal of Physics*, 49(5):606–620.

Ossipov, P. (1997). The angular coefficient method for calculating the stationary molecular gas flow for arbitrary reflection law. *Vacuum*, 48(5):409–412.

Persson, P., Hellborg, R., Kiisk, M., et al. (2003). The pressure profile in the lund pelletron accelerator with the newly installed terminal pumping in use. *Nuclear Instruments and Methods in Physics Research Section A: Accelerators, Spectrometers, Detectors and Associated Equipment*, 500(1-3):55–61.

Pilipenko, D. and Fogel, Y. M. (1962). Electron capture and loss by fast hydrogen atoms passing through molecular gases. *Soviet Phys. JETP*, 15:646.

Prasanth, P. and Kakkassery, J. K. (2008). Molecular models for simulation of rarefied gas flows using direct simulation Monte Carlo method. *Fluid Dynamics Research*, 40(4):233.

Puckett, L., Taylor, G., and Martin, D. (1969). Cross sections for ion and electron production in gases by 0.15-1.00-MeV hydrogen and helium ions and atoms. *Physical Review*, 178(1):271.

Saitoh, Y., Chiba, A., and Narumi, K. (2009). Transmission of cluster ions through a tandem accelerator of several stripper gases. *Review of Scientific Instruments*, 80(10).

Schryber, U. (1967). *Elektroneneinfang schneller protonen in gasen*. PhD thesis, ETH Zurich.

Shima, K., Ishii, S., Takahashi, T., et al. (2001). Optimum thickness of carbon stripper foils in tandem accelerator in view of transmission and lifetime. *Nuclear Instruments and Methods in Physics Research Section A: Accelerators, Spectrometers, Detectors and Associated Equipment*, 460(2-3):233–238.

Shirshekan, M., Hasanpour, O., Sadafi Biabli, M., et al. (2024). Implementation of a control system for a laboratory-scale 1 MeV/25 kW electrostatic accelerator for irradiation experiments. *Radiation Physics and Engineering*.

Sterpin, E., Widesott, L., Poels, K., et al. (2024). Robustness evaluation of pencil beam scanning proton therapy treatment planning: A systematic review. *Radiotherapy and Oncology*, 197:110365.

Stier, P. M. and Barnett, C. (1956). Charge exchange cross sections of hydrogen ions in gases. *Physical Review*, 103(4):896.

Tawara, H. et al. (1990). Some electron detachment data for h-ions in collisions with electrons, ions, atoms and molecules. Technical report, National Inst. for Fusion Science, Nagoya (Japan).

Toburen, L., Nakai, M., and Langley, R. (1968). Measurement of high-energy charge-transfer cross sections for incident protons and atomic hydrogen in various gases. *Physical Review*, 171(1):114.

Uchiyama, T., Agawa, Y., Nishihashi, T., et al. (1991). Electrostatic accelerators with high energy resolution. *Nuclear Instruments and Methods in Physics Research Section B: Beam Interactions with Materials and Atoms*, 56:1036–1038.

Upadhyay, S., Mandal, A., Subrahmanyam, N., et al. (2016). Effects of high-energy proton implantation on the luminescence properties of InAs submonolayer quantum dots. *Journal of Luminescence*, 171:27–32.

Van de Graaff, R. (1960). Tandem electrostatic accelerators. *Nuclear Instruments and Methods*, 8(2):195–202.

von Reden, K., Zhang, M., Meigs, M., et al. (2007). Carbon nanotube foils for electron stripping in tandem accelerators. *Nuclear Instruments and Methods in Physics Research Section B: Beam Interactions with Materials and Atoms*, 261(1-2):44–48.

Welsh, L. M., Berkner, K. H., Kaplan, S. N., et al. (1967). Cross sections for electron capture by fast protons in H2, He, N2, and Ar. *Physical Review*, 158(1):85.

Wiebert, A., Erlandsson, B., Hellborg, R., et al. (1995). The pressure profile in the Lund Pelletron accelerator. *Nuclear Instruments and Methods in Physics Research Section A: Accelerators, Spectrometers, Detectors and Associated Equipment*, 364(2):201–204.

Zarei, S., Davani, F. A., Rachti, M. L., et al. (2017). Design of a side coupled standing wave accelerating tube for NSTRI e-Linac. *Journal of Instrumentation*, 12(09):P09026.

Zarei, S., Ghasemi, F., Hajari, S. S., et al. (2023). Construction and measurement of the prototype side-coupled standing-wave tube for electron linac. *Journal of Instrumentation*, 18(10):T10006.

Zhou, Z., Kato, K., Komaki, T., et al. (2004). Effects of hydrogen doping through ion implantation on the electrical conductivity of ZnO. *International Journal of Hydrogen Energy*, 29(3):323–327.

Zmeškal, M., Košťál, M., Czakoj, T., et al. (2023). Characterization of the secondary neutron field inside a cyclotron for production of radiopharmaceuticals. *Applied Radiation and Isotopes*, 199:110865.

To cite this article:

Mohseni Kejani, M., Abbasi Davani, F., Ghasemi, F., Sanaye Hajari, S. and Lamehi Rachti, M. (2025). Vacuum system design and pressure profile calculation for the accelerating tube of a tandem accelerator. *Radiation Physics and Engineering*, 6(4): 55-64. doi: 10.22034/rpe.2025.534992.1284

DOI: 10.22034/rpe.2025.534992.1284

To link to this article: https://doi.org/10.22034/rpe.2025.534992.1284